Articles

The Adsorption of Methanethiol and Benzenethiol on Silver Surfaces

Kyong-Hoon Lee, Sang-Hyun Park, and Hojing Kim*

Research Institute of Molecular Sciences, Department of Chemistry, Seoul National University, Seoul 151-742, Korea
Received July 16, 1994

The adsorption of methanethiol and benzenethiol on Ag(111) and Ag(100) surfaces is studied respectively, employing ASED (Atom Superposition and Electron Delocalization) method. Metal surfaces are modelled by 3-layer clusters. The corresponding thiolate anions are taken as adsorbates. The highly coordinated binding sites are most favored for both surfaces. The tilted angles of C-S axis from the surface normal are nearly zero. There's Charge transfer from adsorbate to substrate and the stretching frequency of C-S bond upon adsorption is blue-shifted from its gas phase counterpart, and its amount is the smallest at most highly coordinated site. FMO (Fragment Molecular Orbital) analysis of the system give the explanation for these results.

Introduction

Alkanethiol adsorbed on metal surface has been the subject of great interest recently because of its technological applicability both to the formation of Self-Assembled Monolayers[1~13] and to the catalytic desulfurization processes.[14~25]

In general, alkanethiol undergoes its S-H bond cleavage to be adsorbed onto metal surface *via* its sulfur atom in the form of alkylthiolate, though the exact mechanism involved is not yet known. The adsorption orientation angle, however, is characteristic of a system and thus important for identifying the system in terms of chain length[1~5,7] and tail functional group[4,5,8] of the adsorbate, and the metal surface.[8] Especially the dependence of adsorption geometry on the nature of metal surface shows a wide variety and has no known general rules.

One way of coming closer to the principles residing here would be to look into the chemical change devoted to the C-S bond of adsorbate before and after the adsorption.[8~14,23~25] Methanethiol, the simplest of alkanethiol, became representative of the study for this purpose both in experiments[9~11,14~22] and in calculations.[12,13,23~25]

On the other hand, aromatic thiol, which is not drawing so much attention as alkylthiol, provides a different kind of interest to us because it has another electron rich group added to sulfur atom. Benzenethiol, the simplest of this species, would be adequate to see the different role of each functional group when adsorbed to metal surface.

This work is intended to find an equilibrium geometry and then to explain chemistry therein through ASED-MO calculational method upon the respective adsorption of methanethiol and benzenethiol molecule on both surfaces of Ag(111) and Ag(100).

Computational Details

ASED-MO method. In this study, Atom Superposition and Electron Delocalization molecular orbital (ASED-MO)[26,27] calculational method is used. This introduces nuclear repulsion to its predecessor Extended Hückel (EH)[33] so as to find out an equilibrium geometry. It is based on a physical model of partitioning molecular electronic charge density functions into rigid atomic parts that are centered on the unclei and the nonrigid bond charge redistribution part. In equation (1), E_r is a pairwise repulsive energy due to rigid atom superpositon. The forces on the nuclei from bond charge delocalization are attractive and symbolized by E_d so that molecular binding energy E is expressed as

$$E = E_r + E_d \tag{1}$$

It has been found in many studies[27~32] that when the components of E_r are calculated by integrating the force on the uncleus of the less electronegative atom of each pair that is due to the density distribution, including the unclear charge, of the more electronegative atom, E_d is well approximated by a change in electron orbital energy ΔM_{MO} given by

$$\Delta E_{MO} = \sum_i n_i \varepsilon_i^{MO} - \sum_a \sum_i n_i \varepsilon_i^{AO} \tag{2}$$

In equation (2) n_i is the orbital occupation number, ε^{MO} is the valence molecular orbital energy, ε^{AO} is the valence atomic orbital energy, and the sums are over all orbitals i and all atoms a. The ε^{AO} is the negative of valence state ionization potential, VSIP. The ε^{MO} is obtained from a modified extended Hückel (EH) Hamiltonian whose matrix elements are given by equation (3) and (4).

$$H_{ii}^{aa} = -\mathrm{VSIP}_i^a \tag{3}$$

$$H_{ij}^{ab} = 1.125(H_{ii}^{aa} + H_{jj}^{bb}) S_{ij}^{ab} \exp(-0.13 R^{ab}) \tag{4}$$

In equation (4) S_{ij}^{ab} is the overlap integral between atomic orbitals i on atom a and j on atom b and R^{ab} is the distance between the unclei of atoms a and b.

COOP (Crystal Orbital Overlap Population). The Crystal Orbital Overlap population (COOP) curve is a plot of the overlap- population-weighted density of states versus energy.[34] Integration of the COOP curve up to the Fermi energy gives the total overlap population. The positive re-

Table 1. Silver clusters[a] used in this study

	Ag(111)		Ag(100)	
Total Number of Atoms	43	48	41	55
Array of Atoms (3-layer)	19-12-12	18-15-15	16-9-16	24-15-16
Energy per Atom (eV)	−151.76	−151.74	−151.77	−151.77
Fermi Energy (eV)	−10.29	−10.41	−10.38	−10.56

[a]Smaller clusters are used for methylthiolate[39,40] and larger ones for phenylthiolate.

gions of the COOP curve indicate bonding and the negative regions antibonding. The amplitude of the COOP curve depends on the number of states in an energy interval, the magnitude of the coupling overlap, and the size of the coefficients in the MO's.[35] The definition of COOP curve of a bond A-B is given in the equation (5), where c_{ji} is the jth coefficient of ith MO and s_{jk} is an overlap integral of jth atomic orbital and kth atomic orbital.

$$\mathrm{COOP}_{A\text{-}B}=\sum_i 2\delta(E-E_i)\sum_{j\in A}\sum_{k\in B}c_{ji}c_{ki}S_{jk} \tag{5}$$

ROP (Reduced Overlap Population). The Reduced Overlap Population (ROP) of a bond A-B is defined as in equation (6), Where n_i is the occupation number of the ith MO. It has been used successfully as an indication of the strength of a given bond and has been correlated with such properties as force constants, vibrational frequencies, and dissociation energies.[36,37]

$$\mathrm{ROP}_{A\text{-}B}=2\sum_i n_i\sum_{j\in A}\sum_{k\in B}c_{ji}c_{ki}S_{jk} \tag{6}$$

This ROP can be resolved into the contribution from each atomic orbital as follows. The $\mathrm{ROP}_{A\text{-}B}$ (A, p) of equation (7) represents the contribution of p atomic orbital of atom A to A-B bond strength. This can be also resolved into the contribution of each molecular orbital of a given molecule to $\mathrm{ROP}_{A\text{-}B}$ (A, p).

$$\begin{aligned}\mathrm{ROP}_{A\text{-}B}&=2\sum_i n_i\sum_{j\in A,p}\sum_{k\in B}c_{ji}c_{ki}S_{jk}+2\sum_i n_i\sum_{j\in A,q}\sum_{k\in B}c_{ji}c_{ki}S_{jk}\\&\quad+2\sum_i n_i\sum_{j\in A,r}\sum_{k\in B}c_{ji}c_{ki}S_{jk}\\&=\mathrm{ROP}_{A\text{-}B}(A,p)+\mathrm{ROP}_{A\text{-}B}(A,q)+\mathrm{ROP}_{A\text{-}B}(A,r)\end{aligned} \tag{7}$$

FMO (Fragment Molecular Orbital) analysis. To obtain the detailed information on adsorption, Fragment Molecular Orbital (FMO)[38] analysis is carried out. ASED-MO orginally uses an atomic basis set from atoms constituting the system concerned. But FMO instead uses a molecular orbital basis set from fragment molecules composing the system. With the basis set transformation of this kind, it is possible to see the role of each molecular orbital of adsorbate in the formation of chemisorption bond.

Silver Clusters. The cluster models are used for representing Ag(111) and Ag(100) surfaces. For methylthiolate, cluster models from previous works[39,40] are used and the larger clusters are used for phenylthiolate. The details of model clusters are given in Table 1 and their top views are shown in Figures 1 and 2. There're several adsorption sites

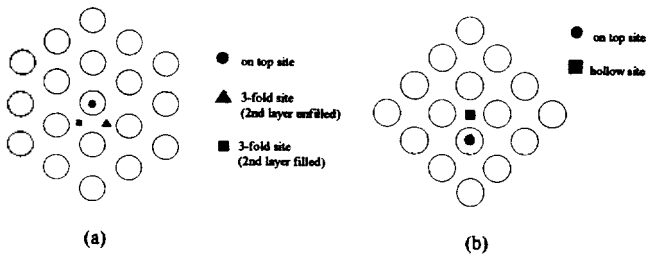

Figure 1. Top view of silver clusters used for methylthiolate in this study (a) Ag(111) (b) Ag(100).

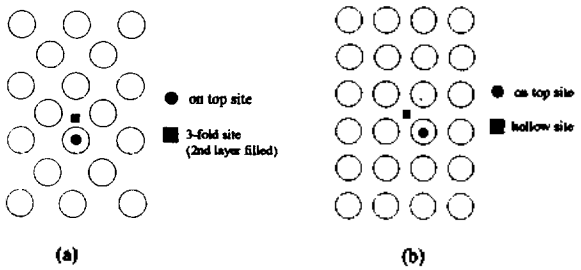

Figure 2. Top view of silver clusters used for phenylthiolate in this study (a) Ag(111) (b) Ag(100).

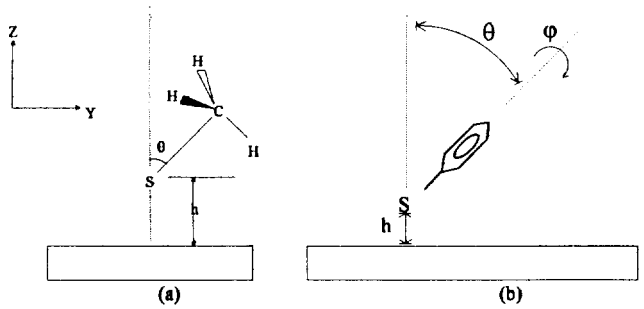

Figure 3. Schematic view of (a) methylthiolate (b) phenylthiolate adsorbed on metal surface.

available for each surface according to the possible location of sulfur atom of the adsorbates. These are shown in Figures 1 and 2. The Ag-Ag distance is set as 2.89 Å, which is the nearest neighbor distance in bulk silver.[45]

Methanethiol and Benzenethiol. Both of methanethiol and benzenethiol undergo their respective S-H bond rupture to be adsorbed onto metal surface *via* the sulfur atom,[1~25,47] and hydrogen gas is evolved as a result of this process. Though the exact mechanism involved is not yet known, adsorbed species are indeed thiolate anions. In this work, methylthiolate and phenylthiolate anions are thus taken as adsorbates.

The geometries of the adsorbates used in this study are obtained through full geometry optimization of the corresponding thiols by PM3 semi-empirical SCF-MO calculational method.[41]

Geometric variables. In Figure 3, schematic views of adsorbates on metal surface is shown. For each adsorption site of each surface, the equilibrium adsorption geometry is obtained by concurrent variation of the height of sulfur atom over the surface (h in Fugure 3), the angle of C-S

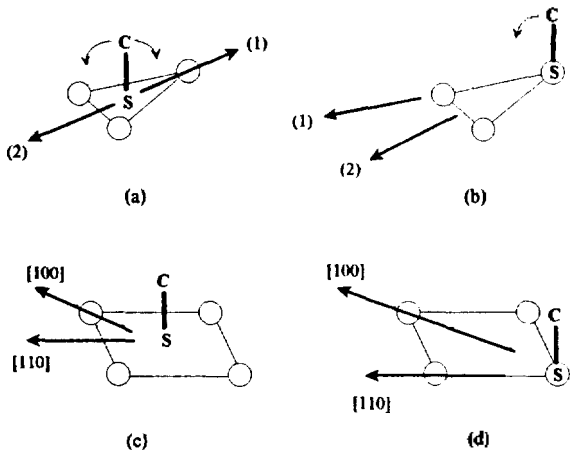

Figure 4. Schematic view of the azimuthal direction of adsorbates set in two modes. Adsorbate is represented only by C-S bond. (a) hollow site at Ag(111) (b) on-top site at Ag(111) (c) hollow site at Ag(100) (d) on-top site at Ag(100).

Table 2. Extended Hückel (EH) parameters[a]

Atom	Orbital	H_{ii} (eV)	ζ_1[b]	ζ_2[b]	c_1[b]	c_2[b]
H	1*s*	−12.10	1.200			
C	2*s*	−15.09	1.658			
	2*p*	−9.76	1.618			
S	3*s*	−20.50	2.022			
	3*p*	−10.66	1.727			
Ag	5*s*	−10.58	2.044			
	5*p*	−6.92	1.744			
	4*d*	−14.00	6.070	2.363	0.5780	0.6252

[a] All the parameters used in this study are from ref. 42 & 43. [b] ζ's are Slater exponents and c's are corresponding linear coefficients.

axis from the surface normal (θ in Figure 3), and the azimuthal direction of the main symmetry axis of adsorbates (in Figure 4).

In the case of phenylthiolate, rotation of phenyl ring about C_2 axis of the phenylthiolate is also considered. This is represented as φ in Figure 3(b).

First, the azimuthal direction of main symmetry axis is set in two modes according to the symmetry of each adsorption site. They are shown in Figure 4. For each azimuthal direction, the height over the surface and the tilt angle of C-S axis are changed by 0.05 Å and by 5° respectively. EH Parameters used in this study are listed in Table 2.

Results and Discussion

Methylthiolate. The Crystal Orbital Overlap Population (COOP) curve of C-S bond and the shapes of molecular orbitals for the free methylthiolate molecule are shown is Figures 5 and 6. From analysis of these figures and coefficients of molecular wavefunctions, some information on the adsorbate can be drawn.

$1a_1$ and $1e$ molecular orbitals are bonding and $2a_1$ antibonding with respect to C-S bond as can be seen in Figure

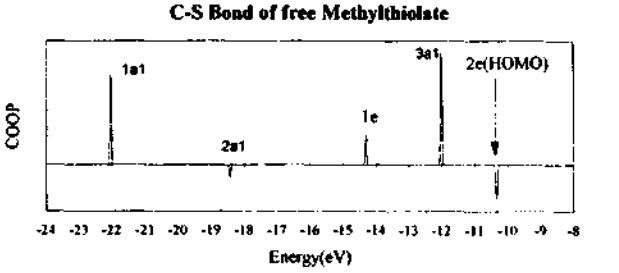

Figure 5. COOP (Crystal Orbital Overlap Population) curve of C-S bond of free methylthiolate molecule.

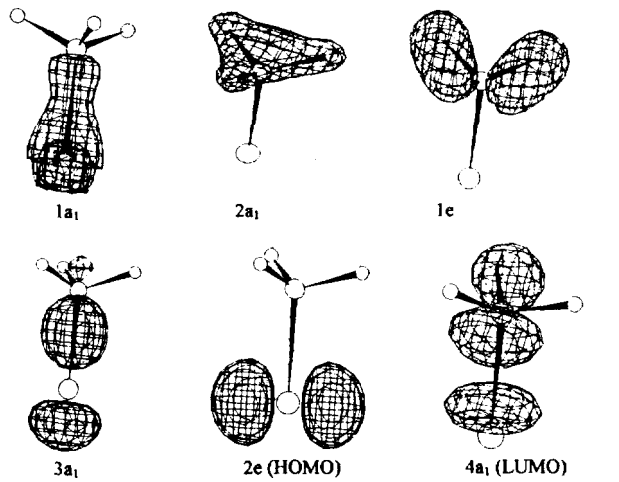

Figure 6. Valence molecular orbitals of free methylthiolate molecule.

5. The contributions of $2a_1$ and $1e$ molecular orbitals to the chemisorption are very small because they have much of methyl group character. $2e$ (HOMO) correspond essentially to ($3p_x$, $3p_y$) orbitals of sulfur. It is nonbonding molecular orbitals with respect to C-S bond with weak antibonding character. $3a_1$ is a C-S bonding orbital and its main atomic components are 3*s* and $3p_z$ atomic orbitals of sulfur.

Tables 3 and 4 show the results of calculations for methylthiolate at each surface, respectively. They can be summarized as follows. First, the overall system is more stable at highly coordinated site and the C-S axis is perpendiculat to metal surface. The values of θ are near 70° for on-top sites, and 0° for hollow sites, respectively. According to SFG (sum frequency generation) spectroscopic experiment of Harris *et al.*,[10,11] C_{3v} axis of methylthiolate is nearly perpendicular to Ag(111) surface. Sellers *et al.*[13] performed an *ab initio* calculation on an nearly identical system. In their work, the calculated values of θ, the angle from the surface normal, are 0° for the hollow and 75° for the on-top.

Second, net charge of the adsorbate indicates that there's charge transfer from the adsorbate to the surface upon adsorption, though it is rather exaggerated in its absolute quantity. The stretching frequency of C-S bond when adsorbed (ROP in Tables 3 and 4) is blue-shifted from its gas phase counterpart at every binding site. This calculated blue-shift of C-S stretching frequency agrees to the result of gas phase experiments,[11,46] but not to that of the solution phase one

Table 3. Optimized adsorption geometries of CH_3S on Ag(111) surface

	az.[a]	*h*[b]	*d*[c]	θ[d]	*BE*[e]	ROP (C-S)[f]	charge[g]
CH_3SH[h]	–	–	–	–	–	0.622	0.00
CH_3S[i]	–	–	–	–	–	0.614	−1.00
on-top	(1)	2.40	2.40	70.0	1.25	0.689	0.78
	(2)	2.40	2.40	65.0	1.24	0.681	0.81
hollow[j]	(1)	1.80	2.46	30.0	1.93	0.645	1.24
(unfilled)	(2)	1.80	2.46	25.0	1.90	0.641	1.17
hollow[k]	(1)	1.75	2.42	0.0	1.97	0.638	1.14
(filled)	(2)	1.75	2.42	10.0	1.98	0.639	1.14

[a]the azimuthal direction, designated in Figure 4. [b]the height of the adsorbate over silver surface (Å), shown in Figure 3. [c]the distance between sulfur atom of the adsorbate and surface (Å). [d]the angle of C-S axis from the surface normal (degree), shown in Figure 3. [e]Binding Energy = Energy (CH_3S^-) + Energy (Ag_{43}) - Energy (total system) (eV). [f]Reduced Overlap Population (C-S bond of the adsorbate). [g]net charge of the adsorbate. [h]the free gas molecule of methanethiol. [i]the free gas molecule of methylthiolate. [j]the hollow site without a silver atom in its center hole (unfilled). [k]the hollow site with a silver atom in its center hole (filled).

Table 4. Optimized adsorption geometries of CH_3S^- on Ag(100) surface

	az.[a]	*h*[b]	*d*[c]	θ[d]	*BE*[e]	ROP[f]	charge[g]
CH_3SH[h]	–	–	–	–	–	0.622	0.00
CH_3S^-[i]	–	–	–	–	–	0.614	−1.00
on-top	[100]	2.40	2.40	75.0	1.64	0.683	0.459
	[110]	2.40	2.40	75.0	1.62	0.703	0.564
hollow	[100]	1.40	2.48	0.0	2.97	0.669	1.25
	[110]	1.40	2.48	5.0	2.97	0.669	1.25

[a]the azimuthal direction, shown in Figure 4. [b]the height of the adsorbate over silver surface (Å), shown in Figure 3. [c]the distance between sulfur atom of the adsorbate and surface (Å). [d]the angle of C-S axis from the surface normal (degree), shown in Figure 3. [e]Binding Energy = Energy (CH_3S^-) + Energy (Ag_{41}) - Energy (total system) (eV). [f]Reduced Overlap Population (C-S bond of the adsorbate). [g]net charge of the adsorbate. [h]the free gas molecule of methanethiol. [i]the free gas molecule of methylthiolate.

in which the red shift is observed.[9] The authors of reference 9 cautiously argues that this discrepancy may come from the hydration effect of a solution medium. The amount of charge transfer is calculated greater at more highly coordinated site and that of blue shift is reciprocally smaller to that extent. This seems to be the same as the SERS (Surface-Enhanced Raman Scattering) result and its theoretical interpretation of Lee *et al.*.[9]

Table 5 and 6 represent how much each molecular orbital of the adsorbate contributes to ROP (Reduced Overlap Population) of the chemisorption bond between adsorbate and substrate, *i.e.* the interaction between adsorbate and substrate in the formation of chemisorption bond. This clearly shows that the chemisorption bond formed here is mainly attributed to 2*e* (HOMO) and $3a_1$ molecular orbitals at every binding site. In other words, the system owes the variation on its geometry and C-S stretching frequency largely to these two molecular orbitals.

HOMO 2*e*, nonbonding but slightly antibonding with respect to C-S bond, always makes the largest contribution to the formation of the chemisorption bond (Tables 5 and 6) and increases its relative role most remarkably as the chemisorption bond becomes stronger through moving from the on-top site to the hollow site by giving more electrons to the surface. This, in turn, means the chemisorption bond is becoming much of π-bonding character with the increase of the coordination number of binding site finally to reach the exact perpendicularity, and at the same time the C-S

Table 5. ROP (CH_2S -Ag_{43}) and the contribution from each MO of CH_3S^- to this value when adsorbed on Ag(111)

	on-top	hollow (u)[a]	hollow (f)[b]
	(1)[c]	(1)[c]	(1)[c]
	θ[d] = 70.0	θ[d] = 30.0	θ[d] = 0.0
ROP (adsorbate-substrate)	.473	1.182	1.346
	contribution from each MO		
$4a_1$ (LUMO)	.000	−.001	−.003
2*e* (HOMO)	.483	.843	.924
$3a_1$	.110	.383	.411
1*e*	−.044	−.031	−.018
$2a_1$	.022	.102	.119
$1a_1$	−.125	−.116	−.088

[a]the hollow site without a silver atom in its hole (unfilled). [b]the hollow site with a silver atom in its hole (filled). [c]the azimuthal angle direction (degree), given in Figure 4. [d]the angle of C-S axis from the surface normal (degree), given in Figure 3.

Table 6. ROP (CH_3S^- -Ag_{41}) and the contribution from each MO of CH_3S to this value when adsorbed on Ag(100)

	on-top	hollow
	[100][a]	[100][a]
	θ[b] = 75.0	θ[b] = 0.0
ROP (adsorbate-substrate)	.408	1.455
	contribution from each MO	
$4a_1$ (LUMO)	.002	.003
2*e* (HOMO)	.454	1.165
$3a_1$	.112	.327
1*e*	−.076	−.035
$2a_1$	.021	.120
$1a_1$	−.122	−.127

[a]the azimuthal angle direction, designated in Figure 4. [b]the angle of C-S axis from the surface normal, designated in Figure 3.

Table 7. Optimized adsorption geometries of $C_6H_5S^-$ on Ag(111) surface

	az.[a]	*h*[b]	*d*[c]	θ[d]	φ[e]	*BE*[f]	ROP (C-S)[g]	charge[h]
C_6H_5SH[i]	–	–	–	–	–	–	0.782	0.00
$C_6H_5S^-$[j]	–	–	–	–	–	–	0.778	−1.00
on-top	(2)	2.45	2.45	85.0	0.0	1.43	0.918	1.86
	(1)	2.45	2.45	85.0	10.0	1.63	0.850	0.80
hollow[k]	(1)	1.80	2.46	0.0	25.0	1.99	0.801	1.40
(filled)	(2)	1.80	2.46	30.0	25.0	2.04	0.802	1.34

[a]the azimuthal direction, designated in Figure 4. [b]the height of the adsorbate over silver surface (Å), designated in Figure 3. [c]the distance between sulfur atom of the adsorbate and surface (Å). [d]the angle of C-S axis from the surface normal (degree), designated in Figure 3. [e]the lying angle of aromatic ring (degree), designated in Figure 3. [f]Binding Energy=Energy ($C_6H_5S^-$)+Energy (Ag_{48})-Energy (total system) (eV). [g]Reduced Overlap Population (C-S bond of the adsorbate). [h]net charge of the adsorbate. [i]the free gas molecule of benzenethiol. [j]the free gas molecule of phenylthiolate. [k]the hollow site with a silver atom in its center hole (filled).

Table 8. Optimized adsorption geometries of $C_6H_5S^-$ on Ag(100) surface

	az.[a]	*h*[b]	*d*[c]	θ[d]	φ[e]	*BE*[f]	ROP[g]	charge[h]
C_6H_5SH[i]	–	–	–	–	–	–	0.782	0.00
$C_6H_5S^-$[j]	–	–	–	–	–	–	0.778	−1.00
on-top	[110]	2.40	2.40	85.0	5.0	1.70	0.858	0.76
	[100]	2.40	2.40	90.0	0.0	1.73	0.843	0.69
hollow	[110]	1.45	2.48	0.0	0.0	2.66	0.795	1.08
	[100]	1.45	2.48	0.0	0.0	2.67	0.795	1.08

[a]the azimuthal direction, designated in Figure 4. [b]the height of the adsorbate over silver surface (Å), designated in Figure 3. [c]the distance between sulfur atom of the adsorbate and surface (Å). [d]the angle of C-S axis from the surface normal (degree), designated in Figure 3. [e]the lying angle of aromatic ring (degree), designated in Figure 3. [f]Binding Energy=Energy ($C_6H_5S^-$)+Energy (Ag_{55})-Energy (total system) (eV). [g]Reduced Overlap Population (C-S bond of the adsorbate). [h]net charge of the adsorbate. [i]the free gas molecule of benzenethiol. [j]the free gas molecule of phenylthiolate.

bond stretching frequency is blue-shifted because of electron donation from antibonding molecular orbital. However, $3a_1$, which behaves in the same mode as HOMO $2e$ but works less, has bonding nature and just decreases the degree of the blue shift as the coordination number increases.

When it comes to the comparison between the adsorptions of two different hollow sites on Ag(111), silver atom right below the hollow site is important to figuring out the system in more detail. If this exists, calculated values of binding energy, C-S stretching frequency, and angle of C-S axis changes more toward the aforementioned trend. This directly indicates that the atom leads to stronger interaction between adsorbate and surface. Table 5 shows that this also can be explained on the same ground as in the relationship between two adsorptions at on-top and hollow site.

As for two metal surfaces, they generally presents the similar qualitative trend in the calculational results. However, since the hollow site at Ag(111) has 3-fold symmetry while at Ag(100) 4-fold symmetry, Ag(100) would provide deeper and wider hole for binding and thus allow stronger interaction of adsorbate with Ag(100) than with Ag(111). This can be easily confirmed by comparing the height of adsorbate over the hollow sites(h) in Tables 3 and 4. Adsorbate is lying lower at on Ag(100) than at on Ag(111). Tables 5 and 6 show that the role HOMO $2e$, which is most important in the adsorption, become conspicuous on Ag(100), which also signs the stronger interaction.

Phenylthiolate. For phenylthiolate, Tables 7 and 8 show the similar calculational results to methylthiolate. The hollow sites are preferred over the on-top as adsorption sites. C-S axis at hollow sites is nearly perpendicular to surface and at on-top sites lies nearly flat. There's net charge transfer from adsorbate to surface and the blue shift is caused to C-S bond of the adsorbate. The amount of the blue shift is smaller for the hollow.

The Crystal Orbital Overlap Population (COOP) curve and the shapes of molecular orbitals for the free phenylthiolate molecule are shown in Figure 7 and 8. All the molecular orbitals of phenylthiolate belong to one of two groups. One is those composed mainly of atomic orbitals of sulfur. The others are those mainly derived from phenyl group with slight incorporation of atomic orbitals of sulfur. $3b_2$ (HOMO), and $6b_1$, just below HOMO in its energy are mainly composed of $3p_y$ and $3p_x$ atomic orbitals of sulfur atom, respectively. Both of $8a_1$ and $7a_1$ consist primarily of $3s$ and $3p_z$ of sulfur atom. $1a_1$, $2a_1$, and $3a_1$, which are very near to core levels, obtain their nature significantly from $3s$ of sulfur atom.

Tables 9 and 10 show the result of FMO analysis on our

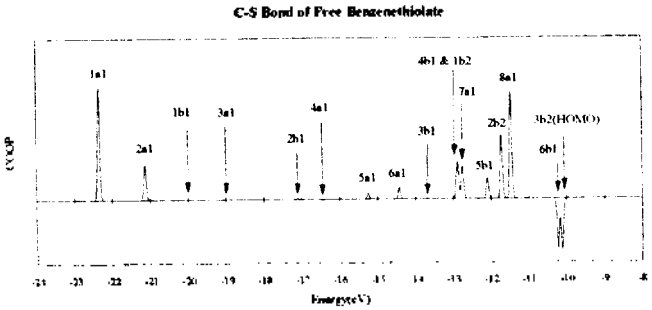

Figure 7. COOP curve of C-S bond of free phenylthiolate molecule.

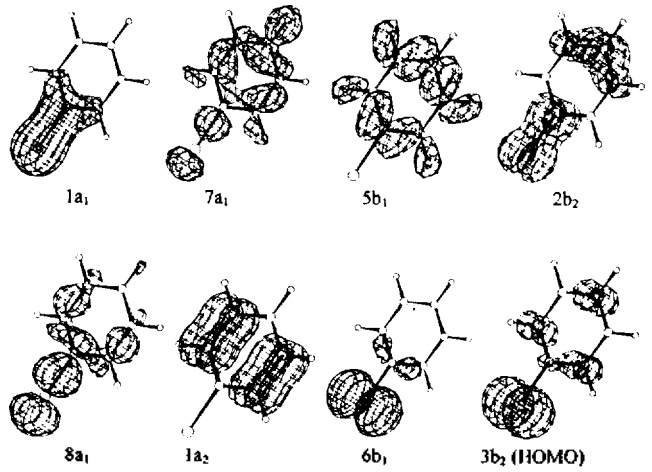

Figure 8. Valence molecular orbitals of free phenylthiolate molecule.

Table 9. ROP (adsorbate-substrate) and difference of the ROP between two different adsorption sites and contribution from each MO of $C_6H_5S^-$ to these values when adsorbed on Ag(111)

	ROP	ΔROP	
	on-top	hollow (f)	from on-top to hollow (f)
TOTAL	.027	1.328	1.301 (100%)
TOTAL	.017	.020	.003 (0.2%)
$2a_2$ (LUMO)	.007	.000	−.007 (−0.5%)
$3b_2$ (HOMO)	.237	.277	.040 (3.1%)
$6b_1$	.144	.435	.291 (22.4%)
$1a_2$	.076	.000	−.076 (−5.8%)
$8a_1$	.041	.242	.201 (15.4%)
$2b_2$	.094	.059	−.035 (−2.7%)
$5b_1$	.006	.016	.010 (0.8%)
$7a_1$	.027	.113	.086 (6.6%)
$1b_2$	−.083	−.006	.077 (5.9%)
$4b_1$	−.002	−.003	−.001 (−0.1%)
$3b_1$	−.005	−.001	.004 (0.3%)
$6a_1$	.006	.033	.027 (2.1%)
$5a_1$	−.017	−.006	.011 (0.8%)
$4a_1$	−.003	.022	.025 (1.9%)
$2b_1$	−.038	−.020	.018 (1.4%)
$3a_1$	−.047	.039	.086 (6.6%)
$1b_1$	−.085	−.015	.070 (5.4%)
$2a_1$	−.110	−.001	.109 (8.4%)
$1a_1$	−.238	.124	.362 (27.8%)

Table 10. ROP (adsorbate-substrate) and difference of the ROP between two different adsorption sites and contribution from each MO of $C_6H_5S^-$ to these values when adsorbed on Ag(100)

	ROP	ΔROP	
	on-top	hollow	from on-top to hollow
	.004	1.352	1.348
MOs above LUMO	.020	.021	.001 (0.0%)
$2a_2$ (LUMO)	.003	.000	−.003 (−0.2%)
$3b_2$ (HOMO)	.311	.432	.121 (9.0%)
$6b_1$	.086	.547	.461 (34.2%)
$1a_2$	.012	.000	−.012 (−0.9%)
$8a_1$	.033	.206	.173 (12.8%)
$2b_2$	.077	.068	−.009 (−0.7%)
$5b_1$	.008	.005	.003 (−0.2%)
$7a_1$	.017	.106	.089 (6.6%)
$1b_2$	−.039	−.003	.036 (2.7%)
$4b_1$	−.002	−.004	−.002 (−0.1%)
$3b_1$	−.007	−.002	.005 (0.4%)
$6a_1$	−.003	.037	.040 (3.0%)
$5a_1$	−.020	.002	.022 (1.6%)
$4a_1$	−.014	.026	.040 (3.0%)
$2b_1$	−.029	−.011	.018 (1.3%)
$3a_1$	−.037	.046	.083 (6.1%)
$1b_1$	−.092	−.004	.088 (6.5%)
$2a_1$	−.105	−.003	.102 (7.6%)
$1a_1$	−.215	.117	.098 (7.3%)

system. At both adsorption sites of on-top and hollow, molecular orbitals largely related with atomic orbitals of sulfur, such as $3b_2$, $6b_1$, $8a_1$, $7a_1$, $3a_1$, $2a_1$, and $1a_1$, play the most important role in the interaction of benzenethiolate with silver surface. On the other hand, molecular orbitals with the nature of the phenyl ring hardly participate in the chemisorption bond.

At on-top sites, total ROP (adsorbate-substrate) seems to represent the very little chance of adsorption. This is largely due to repulsive interaction of molecular orbitals near core levels, especially $1a_1$ and $2a_1$ (minus values in Tables 9 and 10), with surface. They compensate for the attractive interaction by $3b_2$ and $6b_1$. At hollow sites, almost every molecular orbital increases its participation in the interaction so as to markedly strengthen the chemisorption bond compared with at on-top sites. In particular, the difference between these two adsorption characteristics mostly comes from $3b_2$, $6b_1$, $8a_1$, $2a_1$, and $1a_1$. Of these $3b_2$, $6b_1$, and $8a_1$ molecular orbitals just increases the degree of bonding contribution to the chemisorption bond. On the other hand, $2a_1$ and $1a_1$ molecular orbitals, which are very repulsive to the metal surface at on-top sites, lessen their repulsive character or change the mode of the interaction.

Conclusion

The adsorption of methanethiol and benzenethiol on Ag (111) and Ag(100) surface are studied. The equilibrium adsorption geometry and its chemistry is investigated, employing ASED-MO (Atom Superposition and Electron Delocalization) method. The highly coordinated hollow sites are preferred over the on-top as a binding site for both adsorbates on both surfaces. The values of tilted angle of C-S axis from the surface normal at hollow sites are near 0° for both surfaces, whereas at on-top site near 70° for both surfaces. Net charge transfer from adsorbate to surface is calculated and the blue shift is caused to C-S stretching frequency of adsorbed species. The shift is at minimum when adsorbed on hollow sites. It is calculated that the silver atom filled right below the hollow site of Ag(111) plays a role in stabilizing the system in the case of methylthiolate. The equilibrium geometries and their chemistry of methylthiolate and phenylthiolate are determined largely by sulfur atom: in the case of methylthiolate, $2e$ and $3a_1$ molecular orbitals are very important and in the case of phenylthiolate, $3b_2$, $6b_1$, $8a_1$, $2a_1$, and $1a_1$ play an central role.

Acknowledgment. This work has been supported by the Korea Science and Engineering Foundation, the Ministry of Education, the Korea Research Foundation, and the S. N. U. Daewoo Research Fund.

References

1. Nuzzo, R. G.; Zergaski, B. R.; Dubois, L. H. *J. Am. Chem. Soc.* **1987**, *106*, 733.
2. Prime, K. L.; Whitesides, G. M. *Science* **1991**, *252*, 1164.
3. Nuzzo, R. G.; Fusco, F. A.; Allara, D. L. *J. Am. Chem. Soc.* **1987**, *109*, 2358.
4. Porter, M. D.; Bright, T. B.; Allara, D. L.; Chidsey, C. E. D. *J. Am. Chem. Soc.* **1987**, *109*, 3559.
5. Nuzzo, R. G.; Dubois, L. H.; Allara, D. L. *J. Am. Chem. Soc.* **1990**, *112*, 558.
6. Fenter, P.; Eisenberger, P.; Li, J.; Camillone III, N.; Bernasek, S.; Scoles, G.; Ramanarayaman, T. A.; Lang, K. S. *Langmuir* **1991**, *7*, 2013.
7. Bryant, M. A.; Pemberton, J. E. *J. Am. Chem. Soc.* **1991**, *113*, 3629.
8. Walczak, M. M.; Chung, C.; Scott, S.; Stole, M.; Widrig, C. A.; Porter, M. D. *J. Am. Chem. Soc.* **1991**, *113*, 2370.
9. Lee, S. B.; Kim, K.; Kim, M. S.; Oh, W. S.; Lee, Y. S. *J. Mol. Struct.* **1993**, *296*, 5.
10. Harris, A. L.; Rothberg, L.; Dubois, L. H.; Levinos, N. I.; Dhar, L. *Phys. Rev. Lett.* **1990**, *64*, 2086.
11. Harris, A. L.; Rothberg, L.; Dhar, L.; Dubois, L. H.; Levinos, N. I. *J. Chem. Phys.* **1991**, *94*, 2438.
12. Sellers, H. *Surf. Sci.* **1993**, *294*, 99.
13. Sellers, H.; Ulman, A.; Schnidman, Y.; Eilers, J. E. *J. Am. Chem. Soc.* **1993**, *115*, 9389.
14. Albeirt, M. R.; Jiong, P. L.; Bernasek, S. L.; Cameron, S. D.; Gland, J. L. *Surf. Sci.* **1987**, *165*, 251.
15. Castro, M. E.; White, J. M. *Surf. Sci.* **1991**, *257*, 22.
16. Huntley, D. R. *J. Phys. Chem.* **1989**, *93*, 6156.
17. Bao, S.; McConville, C. F.; Woodruff, D. P. *Surf. Sci.* **1987**, *187*, 133.
18. Seymour, D. L.; Bao, S.; McConville, C. F.; Crapper, M. D.; Woodruff, D. P. *Surf. Sci.* **1987**, *189/190*, 520.
19. Sexton, B. A.; Nyberg, G. L. *Surf. Sci.* **1987**, *165*, 251.
20. Wiegand, B. C.; Uvdal, P.; Friend, C. M. *Surf. Sci.* **1992**, *279*, 105.
21. Benziger, J. B.; Preston, R. E. *J. Phys. Chem.* **1989**, *89*, 5002.
22. Rafael, T. S.; Prasad, J.; Fisher, D. A.; Gland, J. L. *Surf. Sci.* **1992**, *278*, 41.
23. Sellers, H. *Surf. Sci.* **1992**, *264*, 177.
24. Rodriguez, J. A. *Surf. Sci.* **1992**, *273*, 385.
25. Rodriguez, J. A. *Surf. Sci.* **1992**, *278*, 326.
26. Anderson, A. B. *J. Chem. Phys.* **1975**, *62*, 1187.
27. Anderson, A. B.; Grimes, R. W.; Hong, S. Y. *J. Phys. Chem.* **1987**, *91*, 4245.
28. Anderson, A. B.; Jen, S.-F. *J. Phys. Chem.* **1990**, *94*, 1607.
29. Anderson, A. B.; Dowd, D. Q. *J. Phys. Chem.* **1987**, *91*, 869.
30. Mehandru, S. P.; Anderson, A. B. *Surf. Sci.* **1988**, *201*, 345.
31. Mehandru, S. P.; Anderson, A. B. *J. Phys. Chem.* **1989**, *93*, 2044.
32. Anderson, A. B.; Awad, M. K. *J. Am. Chem. Soc.* **1985**, *107*, 7854.
33. Hoffmann, R. *J. Chem. Phys.* **1963**, *39*, 1397.
34. Kertesz, M.; Hoffmann, R. *J. Am. Chem. Soc.* **1984**, *106*, 3453.
35. Hoffmann, R. *Rev. Mod. Phys.* **1988**, *60*, 601.
36. Politzer, P.; Kasten, S. D. *J. Phys. Chem.* **1976**, *80*, 385.
37. Kusuma, T. S.; Campanion, A. L. *Surf. Sci.* **1988**, *195*, 59.
38. Howell, J.; Rossi, A.; Wallace, D.; Haraki, K.; Hoffmann, R FORTICON, QCPE No. 344, Indiana University, Bloomington, Indiana, USA.
39. Park, S. H.; Kim, H. *Bull. Korean Chem. Soc.* **1993**, *14*, 244.
40. Hwang, S.; Jang, Y. H.; Kim, H. *Bull. Korean Chem. Soc.* **1991**, *12*, 635.
41. Stewart, J. J. P. *J. Comput. Chem.* **1989**, *10*, 209.
42. Anderson, A. B.; Yu, J. *J. Catal.* **1989**, *119*, 135.
43. Yu, J.; Anderson, A. B. *J. Am. Chem. Soc.* **1990**, *112*, 7219.
44. Bauschlicher Jr., C. W.; Partridge, H.; Langhoff, S. R. *Chem. Phys.* **1990**, *148*, 57.
45. Moruzzi, V. I.; Zanak, J. F.; Williams, A. R. *Calculated Electronic Properties of Metals*; Pergamon Press: New York, U. S. A., 1978, p 148.
46. May, I. W.; Pace, E. L. *Spectrochimica Acta A* **1968**, *24*, 1605.
47. Joo, T. H.; Kim, M. S.; Kim, K. *J. Raman Spectrosc.* **1987**, *18*, 57.